Prediction of nuclear spin based on the behavior of α-particle preformation probability

M. Ismail and A. Adel*
Physics Department, Faculty of Science, Cairo University, Giza, Egypt
(Received 23 September 2013; published 6 November 2013)

A realistic density-dependent nucleon-nucleon (NN) interaction with a finite-range exchange part which produces the nuclear matter saturation curve and the energy dependence of the nucleon-nucleus optical model potential is used to calculate the microscopic α-nucleus potential in the well-established double-folding model. The main effect of antisymmetrization under exchange of nucleons between the α and daughter nuclei has been included in the folding model through the finite-range exchange part of the NN interaction. The α-decay half-lives have been determined using a microscopic potential within the semiclassical Wentzel-Kramers-Brillouin approximation in combination with the Bohr-Sommerfeld quantization condition. We systematically studied the preformation probability, S_α, for ten even-even and odd mass heavy nuclei from Po to No isotopes. We found that S_α has a regular behavior with N if the α particle emitted from adjacent isotopes comes from the same energy levels or from a group of levels, assuming that the order of levels in this group is not changed. Sudden increase in S_α is found when protons and neutrons holes exist below the Fermi levels. Based on the similarity in the behavior of S_α with the neutron number for two adjacent nuclei, we try to determine the unknown or doubted nuclear spins and parities or at least correlate spins of adjacent nuclei.

DOI: 10.1103/PhysRevC.88.054604 PACS number(s): 23.60.+e, 21.10.Tg, 21.10.Jx

I. INTRODUCTION

α decay has long been a useful tool for probing nuclear structure [1–6]. It remains a very important experimental tool for the investigation of unstable nuclei, especially the superheavy ones [7–9]. It can provide information on ground-state lifetime, nuclear interaction, nuclear incompressibility, nuclear spin, and parity [10,11].

The α-decay process is purely a quantum tunneling effect where an α cluster penetrates the Coulomb barrier after its formation in the parent nucleus [12,13]. The barrier penetration probability can easily be obtained from the well-known Wentzel-Kramers-Brillouin (WKB) semiclassical approximation [14]. A reasonable Coulomb barrier is a crucial input for the calculation of the penetration probability and the decay width. The α-nucleus interaction potential consists mainly of both Coulomb repulsive and nuclear attractive parts. These two parts form a barrier between the α particle and the daughter nucleus. The Coulomb component of the potential is well known. In contrast, the nuclear part of the potential is less well defined. There are many different approaches to determine the nuclear part of the α-nucleus interaction potential. It is either introduced phenomenologically [15,16] (e.g., Woods-Saxon shape with adjusted parameters) or generated microscopically in some approximation using calculated nuclear densities [11,17–20] (e.g., the double-folding model).

The experimental data on α-decay half-lives is extensive and being continually updated. A number of theoretical calculations were performed by both phenomenological and microscopic methods to describe α decay and to pursue a microscopic understanding of such phenomenon. The generalized liquid-drop model (GLDM) [21], the density-dependent cluster model (DDCM) [22], the unified model for α decay and α capture [23], the coupled channel approach [24,25], and the Coulomb and proximity potential model [26,27] are in the forefront of the decay study.

In the present work, the α-decay half-lives have been determined using microscopic potential within the semiclassical WKB approximation in combination with the Bohr-Sommerfeld quantization condition. The microscopic α-nucleus potential is numerically constructed in the well-established double-folding model for both Coulomb and nuclear potentials. The main features of the adopted version of the folding model are the inclusion of a realistic density dependence into the effective NN interaction and the explicit treatment of the exchange potential using a realistic local approximation. Therefore, the main effect of antisymmetrization under exchange of nucleons between the α particle and the daughter nucleus has been included in the folding model through the finite-range exchange part of the NN interaction.

The α-spectroscopic factor or the α-preformation probability is investigated in the most theoretical studies through its relation with the α-decay width, and consequently the half-life of heavy nuclei [28]. This is the reason why α decay is an important tool to investigate different nuclear structure effects, such as the valence neutrons and protons, or holes, inside the parent nucleus [29], its isospin asymmetry and its incompressibility [10,30], in addition to the collective vibrational excitations [25] and deformations. The spectroscopic factor, S_α, has been calculated as the ratio of the calculated half-life to the experimentally observed value.

In a previous work [19], we found a correlation between the behavior of S_α with the neutron number and the neutron energy levels of the parent nucleus. We considered in this study the α emission from even neutron number isotopes of the elements Po, Rn, Ra, Th, and U. We found that S_α has a regular behavior with N if the α particle emitted from adjacent isotopes comes from the same energy level or from a group of levels, assuming that the order of levels in this group is not changed. In the

*ahmedshosha200@yahoo.com

present work, we study the α-particle preformation probability for ten even-even and odd mass heavy nuclei with Z in the range $84 \leqslant Z \leqslant 102$. Based on the similarity in the behavior of S_α with the neutron number for two different nuclei, we try to determine the unknown or doubted nuclear spins and parities or at least correlate spins of two different nuclei.

The outline of the paper is as follows. In Sec. II a description of the microscopic nuclear and Coulomb potentials between the α and daughter nuclei is given. The methods for determining the decay width, the penetration probability, the assault frequency, and the preformation probability are also presented. In Sec. III, the calculated results are discussed. Finally, Sec. IV gives a brief conclusion.

II. THEORETICAL FRAMEWORK

Within the density-dependent cluster model (DDCM), the total cluster core potential is composed of nuclear and Coulomb potentials plus the centrifugal part and is given by [11,22]

$$V_{\mathrm{T}}(R) = \lambda\, V_N(R) + V_C(R) + \frac{\hbar^2}{2\,\mu}\frac{\left(\ell+\frac{1}{2}\right)^2}{R^2}, \tag{1}$$

where the renormalization factor λ is the depth of the nuclear potential, R is the separation distance between the mass center of the α particle and the mass center of the core, μ is the reduced mass of the cluster-core system, and ℓ is the angular momentum carried by the α particle.

The nuclear part of the potential $V_N(R)$ consists of two terms, the direct $V_D(R)$ and the exchange $V_{\mathrm{Ex}}(R)$ terms. The direct part of the interaction between two colliding nuclei and the equation describing the Coulomb interaction have similar forms involving only diagonal elements of the density matrix [31,32]

$$V_D(R) = \int d\vec{r}_1 \int d\vec{r}_2 \rho_\alpha(\vec{r}_1)\, \upsilon_D(\rho, E, s)\, \rho_d(\vec{r}_2), \tag{2}$$

where s is the relative distance between a constituent nucleon in the α particle and one in the daughter nucleus. E is the incident laboratory energy per nucleon. $\rho_\alpha(\vec{r}_1)$ and $\rho_d(\vec{r}_2)$ are, respectively, the density distributions of the α particle and the residual daughter nucleus.

The matter density distribution of the α particle is a standard Gaussian form [31], namely,

$$\rho_\alpha(r) = 0.4229\exp(-0.7024\, r^2). \tag{3}$$

The matter density distribution for the daughter nucleus can be described by the spherically symmetric Fermi function [11,22],

$$\rho_d(r) = \frac{\rho_0}{1+\exp\left(\frac{r-R_0}{a}\right)}, \tag{4}$$

where the value of ρ_0 has been fixed by integrating the matter density distribution equivalent to the mass number of the residual daughter nucleus A_d. The half-density radius, R_0, and the diffuseness parameter, a, are given by [11,33,34]

$$R_0 = 1.07\, A_d^{1/3}\mathrm{fm}, \quad a = 0.54\ \mathrm{fm}. \tag{5}$$

The exchange part involves nondiagonal elements of the density matrix and the wave number $k(R)$ associated with the relative motion of the colliding nuclei. The exchange term is, in general, nonlocal. However, an accurate local approximation can be obtained by treating the relative motion locally as a plane wave [35,36],

$$V_{Ex}(E, R) = \int d\vec{r}_1 \int d\vec{r}_2 \rho_\alpha(\vec{r}_1, \vec{r}_1+\vec{s})\, \rho_d(\vec{r}_2, \vec{r}_2-\vec{s}) \times \upsilon_{Ex}(\rho, E, s)\exp\left[\frac{i\vec{k}(R)\cdot\vec{s}}{M}\right], \tag{6}$$

Here $k(R)$ is the relative motion momentum given by

$$k^2(R) = \frac{2\,\mu}{\hbar^2}\left[E_{\mathrm{c.m.}} - V_N(E, R) - V_C(R)\right], \tag{7}$$

where $E_{\mathrm{c.m.}}$ is the center-of-mass energy. $V_N(E, R)$ and $V_C(R)$ are the total nuclear and Coulomb potentials, respectively. The folded potential is energy dependent and nonlocal through its exchange term and contains a self-consistency problem because k depends upon V. The exact treatment of the nonlocal exchange term is complicated numerically, but one may obtain an equivalent *local* potential by using a realistic approximation for the non diagonal density matrix (DM) [37,38]

$$\rho(\vec{r}, \vec{r}+\vec{s}) \simeq \rho\left(\vec{r}+\frac{\vec{s}}{2}\right)\, \hat{j}_1\left(k_{\mathrm{eff}}\left(\vec{r}+\frac{\vec{s}}{2}\right)s\right), \tag{8}$$

with

$$\hat{j}_1(x) = 3\, j_1(x)/x = 3(\sin x - x\, \cos x)/x^3. \tag{9}$$

The α particle is a unique case where a simple Gaussian can reproduce very well its ground state density [31]. Assuming four nucleons to occupy the lowest $s\frac{1}{2}$ harmonic oscillator (h.o.) shell in ^{4}He, one obtains exactly the nondiagonal ground state DM for the α particle as [38,39]

$$\rho_\alpha(\vec{r}, \vec{r}+\vec{s}) = \rho_\alpha\left(\left|\vec{r}+\frac{\vec{s}}{2}\right|\right)\, \exp\left(-\frac{s^2}{4\, b_\alpha^2}\right). \tag{10}$$

The local Fermi momentum $k_{\mathrm{eff}}(r)$ is given by [40,41]

$$k_{\mathrm{eff}}(r) = \left\{\frac{5}{3\rho(r)}\left[\tau(r) - \frac{1}{4}\,\nabla^2\rho(r)\right]\right\}^{1/2}. \tag{11}$$

Using the extended Thomas-Fermi approximation, the kinetic energy density is then given by

$$\tau(r) = \frac{3}{5}\left(\frac{3\pi^2}{2}\right)^{2/3}\, \rho(r)^{5/3} + \frac{1}{3}\nabla^2\rho(r) + \frac{1}{36}\,\frac{|\vec{\nabla}\rho(r)|^2}{\rho(r)}. \tag{12}$$

One easily obtains the self-consistent and local exchange potential V_{Ex} as

$$V_{\mathrm{Ex}}(E, R) = 4\,\pi \int_0^\infty ds\, s^2\, \upsilon_{\mathrm{Ex}}(\rho, E, s)\, j_0(k(E, R)s/M) \times \int d\vec{y}\, \rho_d(|\vec{y}-\vec{R}|)\, \hat{j}_1(k_{\mathrm{eff}}(|\vec{y}-\vec{R}|)s) \times \rho_\alpha(y)\exp\left(-\frac{s^2}{4\, b_\alpha^2}\right). \tag{13}$$

The exchange potential, Eq. (13), can then be evaluated by an iterative procedure which converges very fast.

A realistic NN interaction is used in our calculations whose parameters reproduce consistently the equilibrium density and the binding energy of normal nuclear matter as well as the density and energy dependence of the nucleon-nucleus optical potential. The density dependent M3Y-Paris effective NN force considered in the present work, BDM3Yn, has the factorized form [42]

$$\upsilon_D(\rho, E, s) = \left[11061.625\,\frac{e^{-4s}}{4\,s} - 2537.5\,\frac{e^{-2.5s}}{2.5\,s}\right] F(\rho) g(E), \tag{14}$$

$$\upsilon_{Ex}(\rho, E, s) = \left[-1524.25\,\frac{e^{-4s}}{4\,s} - 518.75\,\frac{e^{-2.5s}}{2.5\,s} - 7.8474\,\frac{e^{-0.7072s}}{0.7072\,s}\right] F(\rho)\, g(E), \tag{15}$$

with the density and energy dependence, respectively,

$$F(\rho) = c(1 - \gamma\rho^n), \tag{16}$$

$$g(E) = (1 - 0.003\,E_{Ap}). \tag{17}$$

The parameters c, γ, and n are adjusted to reproduce normal nuclear matter saturation properties for a given equation of state for cold nuclear matter. For BDM3Y1, $c = 1.2521$, $\gamma = 1.7452\,\mathrm{fm}^3$, and $n = 1$ which generate nuclear matter equation of state with incompressibility value, $K = 270$ MeV [42]. E_{Ap} is the incident energy per projectile nucleon in the laboratory system.

As a next step, the calculated α-daughter nuclear potential will be employed in turn to calculate the α-decay width needed to find the decay half-life. The absolute α-decay width is mainly determined by the barrier penetration probability (P_α), the assault frequency (υ), and the preformation probability, the spectroscopic factor of the α-cluster inside the parent nucleus (S_α), $\Gamma = \hbar\, S_\alpha\, \upsilon\, P_\alpha$. The barrier penetration probability, P_α, could be calculated as the barrier transmission coefficient of the well-known Wentzel-Kramers-Brillouin (WKB) approximation, which works well at energies well below the barrier,

$$P_\alpha = \exp\left(-2\int_{R_2}^{R_3} dr\,\sqrt{\frac{2\,\mu}{\hbar^2}\,|V_T(r) - Q_\alpha|}\right). \tag{18}$$

Here μ is the reduced mass and Q_α is the Q value of the α decay. $R_i (i = 1, 2, 3)$ are the three turning points for the α-daughter potential barrier where $V_T(r)|_{r=R_i} = Q_\alpha$.

The assault frequency of the α particle, υ, can be expressed as the inverse of the time required to traverse the distance back and forth between the first two turning points, R_1 and R_2, as [43]

$$\upsilon = T^{-1} = \frac{\hbar}{2\,\mu}\left[\int_{R_1}^{R_2} \frac{dr}{\sqrt{\frac{2\mu}{\hbar^2}\,|V_T(r) - Q_\alpha|}}\right]^{-1}. \tag{19}$$

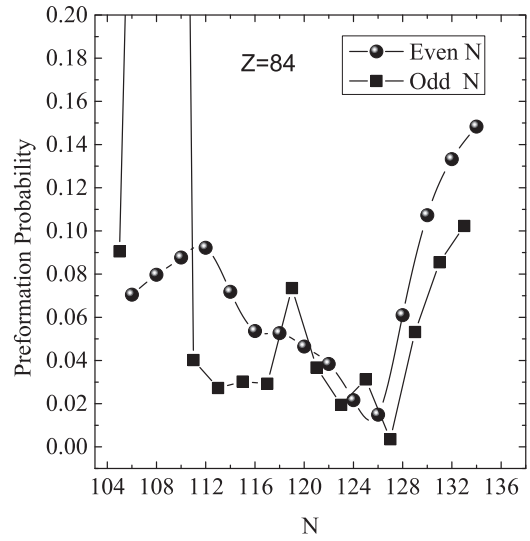

FIG. 1. Extracted α-preformation probability, S_α, using BDM3Y1-Paris NN interactions, for different isotopes of $Z = 84$ with the neutron number N.

The α-decay partial half-lifetime, $T_{1/2}$, of the parent nucleus is given in terms of the α-decay width, Γ, as

$$T_{1/2} = \frac{\hbar \ln 2}{\Gamma}. \tag{20}$$

Finally, the spectroscopic factor (the preformation probability) of the α-cluster inside the parent nucleus can be then obtained as the ratio of the calculated half-life, without S_α, to the experimental one [19,29,30],

$$S_\alpha = T_{1/2}^{\mathrm{cal}} / T_{1/2}^{\mathrm{exp}}. \tag{21}$$

III. RESULTS AND DISCUSSION

Based on the realistic density-dependent effective BDM3Y1-Paris NN interaction, the half-lives of the ground state-to-ground state α-decay of both even-even and odd-A

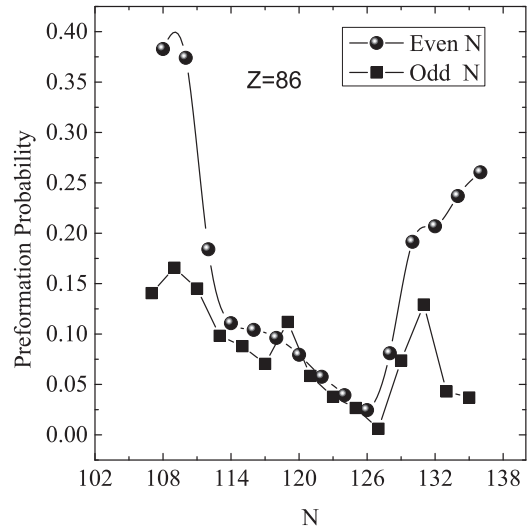

FIG. 2. The same as Fig. 1 but for $Z = 86$.

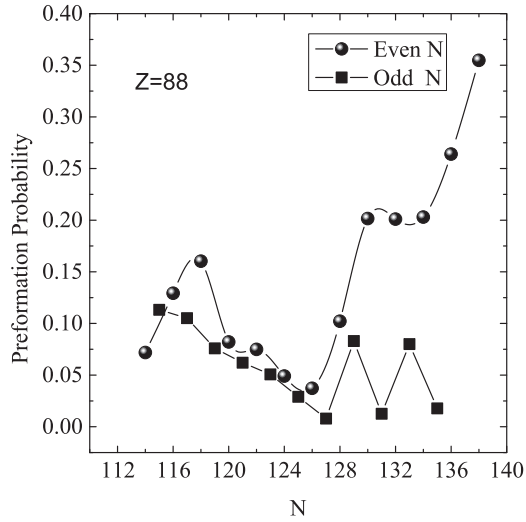

FIG. 3. The same as Fig. 1 but for $Z = 88$.

radioactive nuclei from Po to No isotopes have been calculated. The main effect of antisymmetrization under exchange of nucleons between the α and the daughter nuclei has been included in the folding model through the finite-range exchange part of the NN interaction. We use a realistic NN interaction whose parameters reproduce consistently the equilibrium density and the binding energy of normal nuclear matter as well as the density and energy dependence of the nucleon-nucleus optical potential. This is a novel development in the calculations of α decays.

Above the neutron magic number $N = 126$, Fig. 1 shows that S_α increases almost linearly with increasing the neutron number N. This regular variation of S_α indicates that the neutron pair in α emission comes from the same energy level, also the proton pair is emitted from the same proton level. It is clear on Fig. 1 that for $N > 126$, the neutron and proton pairs occupy the levels $9/2^+$ and $9/2^-$, respectively. The variation of S_α in this neutron variation range confirms that the Bi

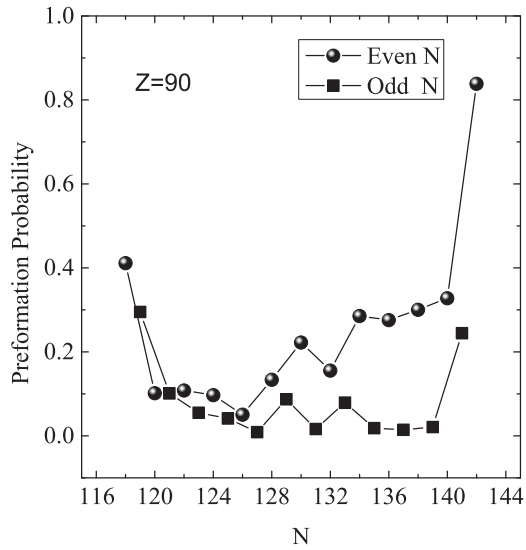

FIG. 4. The same as Fig. 1 but for $Z = 90$.

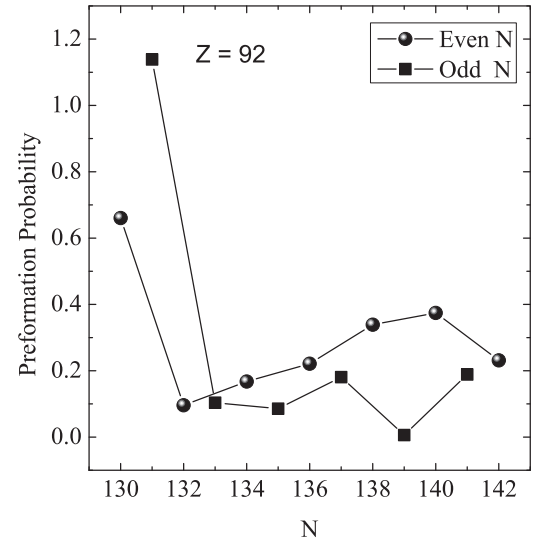

FIG. 5. The same as Fig. 1 but for $Z = 92$.

and At nuclei with $Z = 83$ and 85, respectively, and with even neutron numbers $N = 128$, 130, 132, and 134 have spins $9/2^-$. This means that the linear regular variation of S_α with N for a specific element results from the stability of energy level scheme of this element and its nearest two elements. If the added neutrons above $N = 126$ occupy other level than $9/2^+$, S_α becomes irregular, it decreases or increases with increasing N depending on the spin of the next odd isotope and the stability of proton level scheme against adding or subtracting a proton.

The variation of S_α for odd isotopes is more rapid than for even ones. This is clear on Figs. 2, 3, and 4 for Rn, Ra, and Th isotopes, respectively. The neutron levels above $N = 126$ contributing to the emission process in these three figures are $(9/2^+, 5/2^+, 7/2^+)$, $(9/2^+, 7/2^+, 5/2^+, 3/2^+)$, and $(9/2^+, 7/2^+, 5/2^+, 3/2^+, 1/2^+, 5/2^+)$, respectively, as indicated in Table I. This is compared to only one level $(9/2^+)$ contributes to emission process in Fig. 1.

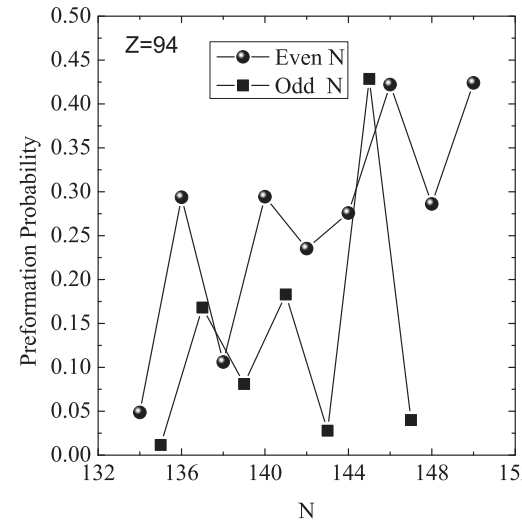

FIG. 6. The same as Fig. 1 but for $Z = 94$.

TABLE I. The preformation probability, S_α, and the α-decay half-lives, $T_{1/2}^{\rm calc}$, calculated without S_α for Po, Rn, Ra, Th, U, Pu, Cm, Cf, Fm, and No isotopes using BDM3Y1-Paris NN interaction. Experimental Q values, α-decay half-lives, spin, and parities are taken from Ref. [44]. Uncertain spin and/or parity assignments are in parentheses.

Reaction	$Q_\alpha^{\rm exp}$ (MeV)	J_i^π	J_f^π	$\ell_{\rm min}$	$T_{1/2}^{\rm exp}$ (s)	$T_{1/2}^{\rm calc}$ (s)	S_α
^{189}Po $\rightarrow$ ^{185}Pb + α	7.6940	$(7/2^-)$	$3/2^-$	2	3.50×10^{-3}	3.17×10^{-4}	0.091
^{190}Po $\rightarrow$ ^{186}Pb + α	7.6930	0^+	0^+	0	2.46×10^{-3}	1.73×10^{-4}	0.071
^{191}Po $\rightarrow$ ^{187}Pb + α	7.493	$(3/2^-)$	$(13/2^+)$	5	2.22×10^{-2}	1.25×10^{-2}	0.562
^{192}Po $\rightarrow$ ^{188}Pb + α	7.3200	0^+	0^+	0	3.24×10^{-2}	2.58×10^{-3}	0.080
^{193}Po $\rightarrow$ ^{189}Pb + α	7.0940	$(13/2^+)$	$(3/2^-)$	5	2.45×10^{-1}	2.98×10^{-1}	1.217
^{194}Po $\rightarrow$ ^{190}Pb + α	6.9870	0^+	0^+	0	3.92×10^{-1}	3.44×10^{-2}	0.088
^{195}Po $\rightarrow$ ^{191}Pb + α	6.7500	$(3/2^-)$	$(3/2^-)$	0	6.19×10^{0}	2.49×10^{-1}	0.040
^{196}Po $\rightarrow$ ^{192}Pb + α	6.6580	0^+	0^+	0	5.92×10^{0}	5.46×10^{1}	0.092
^{197}Po $\rightarrow$ ^{193}Pb + α	6.4120	$(3/2^-)$	$(3/2^-)$	0	1.91×10^{2}	5.20×10^{0}	0.027
^{198}Po $\rightarrow$ ^{194}Pb + α	6.3098	0^+	0^+	0	1.86×10^{2}	1.34×10^{1}	0.072
^{199}Po $\rightarrow$ ^{195}Pb + α	6.0742	$(3/2^-)$	$3/2^-$	0	4.38×10^{3}	1.32×10^{2}	0.030
^{200}Po $\rightarrow$ ^{196}Pb + α	5.9814	0^+	0^+	0	6.22×10^{3}	3.34×10^{2}	0.054
^{201}Po $\rightarrow$ ^{197}Pb + α	5.7989	$3/2^-$	$3/2^-$	0	8.28×10^{4}	2.42×10^{3}	0.029
^{202}Po $\rightarrow$ ^{198}Pb + α	5.7010	0^+	0^+	0	1.39×10^{5}	7.34×10^{3}	0.053
^{203}Po $\rightarrow$ ^{199}Pb + α	5.4960	$5/2^-$	$3/2^-$	2	2.00×10^{6}	1.47×10^{5}	0.074
^{204}Po $\rightarrow$ ^{200}Pb + α	5.4848	0^+	0^+	0	1.89×10^{6}	8.78×10^{4}	0.046
^{205}Po $\rightarrow$ ^{201}Pb + α	5.3250	$5/2^-$	$5/2^-$	0	1.57×10^{7}	5.76×10^{5}	0.037
^{206}Po $\rightarrow$ ^{202}Pb + α	5.3270	0^+	0^+	0	1.40×10^{7}	5.37×10^{5}	0.038
^{207}Po $\rightarrow$ ^{203}Pb + α	5.2158	$5/2^-$	$5/2^-$	0	1.04×10^{8}	2.03×10^{6}	0.019
^{208}Po $\rightarrow$ ^{204}Pb + α	5.2153	0^+	0^+	0	9.15×10^{7}	1.98×10^{6}	0.022
^{209}Po $\rightarrow$ ^{205}Pb + α	4.9792	$1/2^-$	$5/2^-$	2	3.23×10^{9}	1.01×10^{8}	0.031
^{210}Po $\rightarrow$ ^{206}Pb + α	5.4075	0^+	0^+	0	1.20×10^{7}	1.79×10^{5}	0.015
^{211}Po $\rightarrow$ ^{207}Pb + α	7.5945	$9/2^+$	$1/2^-$	5	5.16×10^{-1}	1.85×10^{-3}	0.004
^{212}Po $\rightarrow$ ^{208}Pb + α	8.9541	0^+	0^+	0	2.99×10^{-7}	1.83×10^{-8}	0.061
^{213}Po $\rightarrow$ ^{209}Pb + α	8.5360	$9/2^+$	$9/2^+$	0	3.72×10^{-6}	1.98×10^{-7}	0.053
^{214}Po $\rightarrow$ ^{210}Pb + α	7.8335	0^+	0^+	0	1.64×10^{-4}	1.76×10^{-5}	0.107
^{215}Po $\rightarrow$ ^{211}Pb + α	7.5263	$9/2^+$	$9/2^+$	0	1.78×10^{-3}	1.52×10^{-4}	0.086
^{216}Po $\rightarrow$ ^{212}Pb + α	6.9062	0^+	0^+	0	1.45×10^{-1}	1.93×10^{-2}	0.133
^{217}Po $\rightarrow$ ^{213}Pb + α	6.6621	$(9/2^+)$	$(9/2^+)$	0	1.53×10^{0}	1.57×10^{-1}	0.102
^{218}Po $\rightarrow$ ^{214}Pb + α	6.1147	0^+	0^+	0	1.86×10^{2}	2.76×10^{1}	0.148
^{193}Rn $\rightarrow$ ^{189}Po + α	8.0400	$(3/2^-)$	$(7/2^-)$	2	1.15×10^{-3}	1.62×10^{-4}	0.141
^{194}Rn $\rightarrow$ ^{190}Po + α	7.8620	0^+	0^+	0	7.80×10^{-4}	2.99×10^{-4}	0.383
^{195}Rn $\rightarrow$ ^{191}Po + α	7.6900	$3/2^-$	$(3/2^-)$	0	6.00×10^{-3}	9.95×10^{-4}	0.166
^{196}Rn $\rightarrow$ ^{192}Po + α	7.6170	0^+	0^+	0	4.40×10^{-3}	1.65×10^{-3}	0.374
^{197}Rn $\rightarrow$ ^{193}Po + α	7.4110	$(3/2^-)$	$(3/2^-)$	0	5.30×10^{-2}	7.69×10^{-3}	0.145
^{198}Rn $\rightarrow$ ^{194}Po + α	7.3490	0^+	0^+	0	6.50×10^{-2}	1.20×10^{-2}	0.184
^{199}Rn $\rightarrow$ ^{195}Po + α	7.1400	$(3/2^-)$	$(3/2^-)$	0	6.28×10^{-1}	6.17×10^{-2}	0.098
^{200}Rn $\rightarrow$ ^{196}Po + α	7.0433	0^+	0^+	0	1.20×10^{0}	1.33×10^{-1}	0.111
^{201}Rn $\rightarrow$ ^{197}Po + α	6.8607	$(3/2^-)$	$(3/2^-)$	0	7.00×10^{0}	6.16×10^{-1}	0.088
^{202}Rn $\rightarrow$ ^{198}Po + α	6.7737	0^+	0^+	0	1.24×10^{1}	1.30×10^{0}	0.104
^{203}Rn $\rightarrow$ ^{199}Po + α	6.6298	$(3/2^-)$	$(3/2^-)$	0	6.67×10^{1}	4.69×10^{0}	0.070
^{204}Rn $\rightarrow$ ^{200}Po + α	6.5464	0^+	0^+	0	1.03×10^{2}	9.91×10^{0}	0.096
^{205}Rn $\rightarrow$ ^{201}Po + α	6.3900	$5/2^-$	$3/2^-$	2	6.91×10^{2}	7.74×10^{1}	0.112
^{206}Rn $\rightarrow$ ^{202}Po + α	6.3838	0^+	0^+	0	5.49×10^{2}	4.36×10^{1}	0.079
^{207}Rn $\rightarrow$ ^{203}Po + α	6.2511	$5/2^-$	$5/2^-$	0	2.64×10^{3}	1.54×10^{2}	0.058
^{208}Rn $\rightarrow$ ^{204}Po + α	6.2607	0^+	0^+	0	2.36×10^{3}	1.36×10^{2}	0.058
^{209}Rn $\rightarrow$ ^{205}Po + α	6.1555	$5/2^-$	$5/2^-$	0	1.01×10^{4}	3.80×10^{2}	0.038
^{210}Rn $\rightarrow$ ^{206}Po + α	6.1589	0^+	0^+	0	9.00×10^{3}	3.55×10^{2}	0.039
^{211}Rn $\rightarrow$ ^{207}Po + α	5.9654	$1/2^-$	$5/2^-$	2	1.92×10^{5}	5.12×10^{3}	0.027
^{212}Rn $\rightarrow$ ^{208}Po + α	6.3850	0^+	0^+	0	1.43×10^{3}	3.52×10^{1}	0.025
^{213}Rn $\rightarrow$ ^{209}Po + α	8.2430	$(9/2^+)$	$1/2^-$	5	1.95×10^{-2}	1.18×10^{-4}	0.006
^{214}Rn $\rightarrow$ ^{210}Po + α	9.2080	0^+	0^+	0	2.70×10^{-7}	2.19×10^{-8}	0.081
^{215}Rn $\rightarrow$ ^{211}Po + α	8.8390	$9/2^+$	$9/2^+$	0	2.30×10^{-6}	1.70×10^{-7}	0.074
^{216}Rn $\rightarrow$ ^{212}Po + α	8.1970	0^+	0^+	0	4.50×10^{-5}	8.62×10^{-6}	0.192
^{217}Rn $\rightarrow$ ^{213}Po + α	7.8870	$9/2^+$	$9/2^+$	0	5.40×10^{-4}	6.98×10^{-5}	0.129
^{218}Rn $\rightarrow$ ^{214}Po + α	7.2625	0^+	0^+	0	3.5×10^{-2}	7.25×10^{-3}	0.207

TABLE I. (*Continued*.)

Reaction	$Q_\alpha^{\rm exp}$ (MeV)	J_i^π	J_f^π	$\ell_{\rm min}$	$T_{1/2}^{\rm exp}$ (s)	$T_{1/2}^{\rm calc}$ (s)	S_α
^{219}Rn $\rightarrow$ ^{215}Po + α	6.9461	$5/2^+$	$9/2^+$	2	3.96×10^{0}	1.71×10^{-1}	0.043
^{220}Rn $\rightarrow$ ^{216}Po + α	6.4047	0^+	0^+	0	5.56×10^{1}	1.32×10^{1}	0.237
^{221}Rn $\rightarrow$ ^{217}Po + α	6.1625	$7/2^+$	$(9/2^+)$	2	6.82×10^{3}	2.52×10^{2}	0.037
^{222}Rn $\rightarrow$ ^{218}Po + α	5.5903	0^+	0^+	0	3.30×10^{5}	8.60×10^{4}	0.260
^{202}Ra $\rightarrow$ ^{198}Rn + α	7.8970	0^+	0^+	0	1.60×10^{-2}	1.15×10^{-3}	0.072
^{203}Ra $\rightarrow$ ^{199}Rn + α	7.7400	$(3/2^-)$	$(3/2^-)$	0	3.10×10^{-2}	3.51×10^{-3}	0.113
^{204}Ra $\rightarrow$ ^{200}Rn + α	7.6370	0^+	0^+	0	5.70×10^{-2}	7.37×10^{-3}	0.129
^{205}Ra $\rightarrow$ ^{201}Rn + α	7.4900	$(3/2^-)$	$(3/2^-)$	0	2.10×10^{-1}	2.21×10^{-2}	0.105
^{206}Ra $\rightarrow$ ^{202}Rn + α	7.4150	0^+	0^+	0	2.40×10^{-1}	3.85×10^{-2}	0.160
^{207}Ra $\rightarrow$ ^{203}Rn + α	7.2700	$(3/2^-)$	$(3/2^-)$	0	1.57×10^{0}	1.19×10^{-1}	0.076
^{208}Ra $\rightarrow$ ^{204}Rn + α	7.2730	0^+	0^+	0	1.37×10^{0}	1.12×10^{-1}	0.082
^{209}Ra $\rightarrow$ ^{205}Rn + α	7.1430	$5/2^-$	$5/2^-$	0	5.11×10^{0}	3.17×10^{-1}	0.062
^{210}Ra $\rightarrow$ ^{206}Rn + α	7.1510	0^+	0^+	0	3.85×10^{0}	2.89×10^{-1}	0.075
^{211}Ra $\rightarrow$ ^{207}Rn + α	7.0420	$5/2^{(-)}$	$5/2^-$	0	1.40×10^{1}	7.09×10^{-1}	0.051
^{212}Ra $\rightarrow$ ^{208}Rn + α	7.0316	0^+	0^+	0	1.53×10^{1}	7.51×10^{-1}	0.049
^{213}Ra $\rightarrow$ ^{209}Rn + α	6.8618	$1/2^-$	$5/2^-$	2	2.05×10^{2}	5.95×10^{0}	0.029
^{214}Ra $\rightarrow$ ^{210}Rn + α	7.2730	0^+	0^+	0	2.46×10^{0}	9.20×10^{-2}	0.037
^{215}Ra $\rightarrow$ ^{211}Rn + α	8.8640	$(9/2^+)$	$1/2^-$	5	1.55×10^{-3}	1.23×10^{-5}	0.008
^{216}Ra $\rightarrow$ ^{212}Rn + α	9.5260	0^+	0^+	0	1.82×10^{-7}	1.86×10^{-8}	0.102
^{217}Ra $\rightarrow$ ^{213}Rn + α	9.1610	$(9/2^+)$	$(9/2^+)$	0	1.60×10^{-6}	1.33×10^{-7}	0.083
^{218}Ra $\rightarrow$ ^{214}Rn + α	8.5460	0^+	0^+	0	2.52×10^{-5}	5.08×10^{-6}	0.202
^{219}Ra $\rightarrow$ ^{215}Rn + α	8.1380	$(7/2)^+$	$9/2^+$	2	1.00×10^{-2}	1.26×10^{-4}	0.013
^{220}Ra $\rightarrow$ ^{216}Rn + α	7.5920	0^+	0^+	0	1.80×10^{-2}	3.62×10^{-3}	0.201
^{221}Ra $\rightarrow$ ^{217}Rn + α	6.8804	$5/2^+$	$9/2^+$	2	2.80×10^{1}	2.24×10^{0}	0.080
^{222}Ra $\rightarrow$ ^{218}Rn + α	6.6790	0^+	0^+	0	3.80×10^{1}	7.71×10^{0}	0.203
^{223}Ra $\rightarrow$ ^{219}Rn + α	5.9790	$3/2^+$	$5/2^+$	2	9.88×10^{5}	1.76×10^{4}	0.018
^{224}Ra $\rightarrow$ ^{220}Rn + α	5.7888	0^+	0^+	0	3.14×10^{5}	8.28×10^{4}	0.264
^{226}Ra $\rightarrow$ ^{222}Rn + α	4.8706	0^+	0^+	0	5.05×10^{10}	1.79×10^{10}	0.355
^{208}Th $\rightarrow$ ^{204}Ra + α	8.2000	0^+	0^+	0	1.70×10^{-3}	7.00×10^{-4}	0.411
^{209}Th $\rightarrow$ ^{205}Ra + α	8.2700	$(5/2^-)$	$(3/2^-)$	2	2.50×10^{-3}	7.38×10^{-4}	0.295
^{210}Th $\rightarrow$ ^{206}Ra + α	8.0690	0^+	0^+	0	1.62×10^{-2}	1.65×10^{-3}	0.102
^{211}Th $\rightarrow$ ^{207}Ra + α	7.9400	$(5/2^-)$	$(5/2^-)$	0	4.00×10^{-2}	4.05×10^{-3}	0.101
^{212}Th $\rightarrow$ ^{208}Ra + α	7.9580	0^+	0^+	0	3.17×10^{-2}	3.43×10^{-3}	0.108
^{213}Th $\rightarrow$ ^{209}Ra + α	7.8400	$(5/2^-)$	$5/2^-$	0	1.44×10^{-1}	7.94×10^{-3}	0.055
^{214}Th $\rightarrow$ ^{210}Ra + α	7.8270	0^+	0^+	0	8.70×10^{-2}	8.46×10^{-3}	0.097
^{215}Th $\rightarrow$ ^{211}Ra + α	7.6650	$(1/2^-)$	$5/2^{(-)}$	2	1.20×10^{0}	4.97×10^{-2}	0.041
^{216}Th $\rightarrow$ ^{212}Ra + α	8.0720	0^+	0^+	0	2.60×10^{-2}	1.31×10^{-3}	0.050
^{217}Th $\rightarrow$ ^{213}Ra + α	9.4350	$(9/2^+)$	$1/2^-$	5	2.41×10^{-4}	2.17×10^{-6}	0.009
^{218}Th $\rightarrow$ ^{214}Ra + α	9.8490	0^+	0^+	0	1.17×10^{-7}	1.57×10^{-8}	0.134
^{219}Th $\rightarrow$ ^{215}Ra + α	9.5100	$(9/2^+)$	$(9/2^+)$	0	1.05×10^{-6}	9.16×10^{-8}	0.087
^{220}Th $\rightarrow$ ^{216}Ra + α	8.9530	0^+	0^+	0	9.70×10^{-6}	2.16×10^{-6}	0.222
^{221}Th $\rightarrow$ ^{217}Ra + α	8.6260	$(7/2^+)$	$(9/2^+)$	2	1.68×10^{-3}	2.75×10^{-5}	0.016
^{222}Th $\rightarrow$ ^{218}Ra + α	8.1270	0^+	0^+	0	2.80×10^{-3}	4.35×10^{-4}	0.155
^{223}Th $\rightarrow$ ^{219}Ra + α	7.5670	$(5/2)^+$	$(7/2)^+$	2	6.00×10^{-1}	4.76×10^{-2}	0.079
^{224}Th $\rightarrow$ ^{220}Ra + α	7.2980	0^+	0^+	0	8.10×10^{-1}	2.31×10^{-1}	0.285
^{225}Th $\rightarrow$ ^{221}Ra + α	6.9214	$(3/2^+)$	$5/2^+$	2	5.83×10^{2}	1.07×10^{1}	0.018
^{226}Th $\rightarrow$ ^{222}Ra + α	6.4509	0^+	0^+	0	1.83×10^{3}	5.06×10^{2}	0.276
^{227}Th $\rightarrow$ ^{223}Ra + α	6.1466	$1/2^+$	$3/2^+$	2	1.61×10^{6}	2.32×10^{4}	0.014
^{228}Th $\rightarrow$ ^{224}Ra + α	5.5201	0^+	0^+	0	6.03×10^{7}	1.81×10^{7}	0.301
^{229}Th $\rightarrow$ ^{225}Ra + α	5.1676	$5/2^+$	$1/2^+$	2	2.50×10^{11}	5.27×10^{9}	0.021
^{230}Th $\rightarrow$ ^{226}Ra + α	4.7698	0^+	0^+	0	2.38×10^{12}	7.80×10^{11}	0.328
^{231}Th $\rightarrow$ ^{227}Ra + α	4.2132	$5/2^+$	$3/2^+$	2	2.30×10^{17}	5.61×10^{16}	0.244
^{232}Th $\rightarrow$ ^{228}Ra + α	4.0816	0^+	0^+	0	4.42×10^{17}	3.71×10^{17}	0.839
^{222}U $\rightarrow$ ^{218}Th + α	9.4300	0^+	0^+	0	1.00×10^{-6}	6.61×10^{-7}	0.661
^{223}U $\rightarrow$ ^{219}Th + α	8.9400	$(7/2^+)$	$(9/2^+)$	2	1.80×10^{-5}	2.05×10^{-5}	1.139
^{224}U $\rightarrow$ ^{220}Th + α	8.6200	0^+	0^+	0	9.00×10^{-4}	8.65×10^{-5}	0.096
^{225}U $\rightarrow$ ^{221}Th + α	8.0150	$(5/2^+)$	$(7/2^+)$	2	9.50×10^{-2}	9.84×10^{-3}	0.104
^{226}U $\rightarrow$ ^{222}Th + α	7.7010	0^+	0^+	0	3.50×10^{-1}	5.86×10^{-2}	0.168

TABLE I. (*Continued*.)

Reaction	$Q_\alpha^{\rm exp}$ (MeV)	J_i^π	J_f^π	$\ell_{\rm min}$	$T_{1/2}^{\rm exp}$ (s)	$T_{1/2}^{\rm calc}$ (s)	S_α
$^{227}\mathrm{U} \rightarrow {}^{223}\mathrm{Th} + \alpha$	7.2110	$(3/2^+)$	$(5/2)^+$	2	6.60×10^{1}	5.66×10^{0}	0.086
$^{228}\mathrm{U} \rightarrow {}^{224}\mathrm{Th} + \alpha$	6.8040	0^+	0^+	0	5.75×10^{2}	1.27×10^{2}	0.221
$^{229}\mathrm{U} \rightarrow {}^{225}\mathrm{Th} + \alpha$	6.4750	$(3/2^+)$	$(3/2^+)$	0	1.74×10^{4}	3.15×10^{3}	0.181
$^{230}\mathrm{U} \rightarrow {}^{226}\mathrm{Th} + \alpha$	5.9927	0^+	0^+	0	1.80×10^{6}	6.09×10^{5}	0.339
$^{231}\mathrm{U} \rightarrow {}^{227}\mathrm{Th} + \alpha$	5.5763	$(5/2^-)$	$1/2^+$	3	9.07×10^{9}	5.61×10^{7}	0.006
$^{232}\mathrm{U} \rightarrow {}^{228}\mathrm{Th} + \alpha$	5.4136	0^+	0^+	0	2.17×10^{9}	8.14×10^{8}	0.374
$^{233}\mathrm{U} \rightarrow {}^{229}\mathrm{Th} + \alpha$	4.9086	$5/2^+$	$5/2^+$	0	5.02×10^{12}	9.48×10^{11}	0.189
$^{234}\mathrm{U} \rightarrow {}^{230}\mathrm{Th} + \alpha$	4.8577	0^+	0^+	0	7.75×10^{12}	1.79×10^{12}	0.231
$^{228}\mathrm{Pu} \rightarrow {}^{224}\mathrm{U} + \alpha$	7.9400	0^+	0^+	0	1.10×10^{0}	5.35×10^{-2}	0.049
$^{229}\mathrm{Pu} \rightarrow {}^{225}\mathrm{U} + \alpha$	7.5900	$(3/2^+)$	$(5/2^+)$	2	1.34×10^{2}	1.56×10^{0}	0.012
$^{230}\mathrm{Pu} \rightarrow {}^{226}\mathrm{U} + \alpha$	7.1800	0^+	0^+	0	1.02×10^{2}	3.00×10^{1}	0.294
$^{231}\mathrm{Pu} \rightarrow {}^{227}\mathrm{U} + \alpha$	6.8390	$(3/2^+)$	$(3/2^+)$	0	3.97×10^{3}	6.68×10^{2}	0.168
$^{232}\mathrm{Pu} \rightarrow {}^{228}\mathrm{U} + \alpha$	6.7160	0^+	0^+	0	2.03×10^{4}	2.15×10^{3}	0.106
$^{233}\mathrm{Pu} \rightarrow {}^{229}\mathrm{U} + \alpha$	6.4200	$(5/2^+)$	$(3/2^+)$	2	1.05×10^{6}	8.48×10^{4}	0.081
$^{234}\mathrm{Pu} \rightarrow {}^{230}\mathrm{U} + \alpha$	6.3100	0^+	0^+	0	5.28×10^{5}	1.55×10^{5}	0.294
$^{235}\mathrm{Pu} \rightarrow {}^{231}\mathrm{U} + \alpha$	5.9510	$(5/2^+)$	$(5/2^-)$	1	5.42×10^{7}	9.92×10^{6}	0.183
$^{236}\mathrm{Pu} \rightarrow {}^{232}\mathrm{U} + \alpha$	5.8671	0^+	0^+	0	9.02×10^{7}	2.12×10^{7}	0.235
$^{237}\mathrm{Pu} \rightarrow {}^{233}\mathrm{U} + \alpha$	5.7483	$7/2^-$	$5/2^+$	1	3.91×10^{9}	1.09×10^{8}	0.028
$^{238}\mathrm{Pu} \rightarrow {}^{234}\mathrm{U} + \alpha$	5.5932	0^+	0^+	0	2.77×10^{9}	7.63×10^{8}	0.276
$^{239}\mathrm{Pu} \rightarrow {}^{235}\mathrm{U} + \alpha$	5.2445	$1/2^+$	$7/2^-$	3	7.61×10^{11}	3.26×10^{11}	0.429
$^{240}\mathrm{Pu} \rightarrow {}^{236}\mathrm{U} + \alpha$	5.2558	0^+	0^+	0	2.07×10^{11}	8.74×10^{10}	0.422
$^{241}\mathrm{Pu} \rightarrow {}^{237}\mathrm{U} + \alpha$	5.1400	$5/2^+$	$1/2^+$	2	1.81×10^{13}	7.23×10^{11}	0.040
$^{242}\mathrm{Pu} \rightarrow {}^{238}\mathrm{U} + \alpha$	4.9845	0^+	0^+	0	1.18×10^{13}	3.39×10^{12}	0.286
$^{244}\mathrm{Pu} \rightarrow {}^{240}\mathrm{U} + \alpha$	4.6655	0^+	0^+	0	2.53×10^{15}	1.07×10^{15}	0.424
$^{238}\mathrm{Cm} \rightarrow {}^{234}\mathrm{Pu} + \alpha$	6.6700	0^+	0^+	0	2.30×10^{5}	2.52×10^{4}	0.109
$^{241}\mathrm{Cm} \rightarrow {}^{237}\mathrm{Pu} + \alpha$	6.1852	$1/2^+$	$7/2^-$	3	2.83×10^{8}	1.35×10^{7}	0.048
$^{242}\mathrm{Cm} \rightarrow {}^{238}\mathrm{Pu} + \alpha$	6.2156	0^+	0^+	0	1.41×10^{7}	3.08×10^{6}	0.219
$^{243}\mathrm{Cm} \rightarrow {}^{239}\mathrm{Pu} + \alpha$	6.1688	$5/2^+$	$1/2^+$	2	9.21×10^{8}	8.70×10^{6}	0.009
$^{244}\mathrm{Cm} \rightarrow {}^{240}\mathrm{Pu} + \alpha$	5.9017	0^+	0^+	0	5.71×10^{8}	1.10×10^{8}	0.193
$^{245}\mathrm{Cm} \rightarrow {}^{241}\mathrm{Pu} + \alpha$	5.6230	$7/2^+$	$5/2^+$	2	2.66×10^{11}	9.18×10^{9}	0.035
$^{246}\mathrm{Cm} \rightarrow {}^{242}\mathrm{Pu} + \alpha$	5.4751	0^+	0^+	0	1.49×10^{11}	4.00×10^{10}	0.269
$^{247}\mathrm{Cm} \rightarrow {}^{243}\mathrm{Pu} + \alpha$	5.3530	$9/2^-$	$7/2^+$	1	4.92×10^{14}	2.49×10^{11}	0.001
$^{248}\mathrm{Cm} \rightarrow {}^{244}\mathrm{Pu} + \alpha$	5.1617	0^+	0^+	0	1.20×10^{13}	2.68×10^{12}	0.223
$^{240}\mathrm{Cf} \rightarrow {}^{236}\mathrm{Cm} + \alpha$	7.7110	0^+	0^+	0	6.50×10^{1}	1.07×10^{1}	0.165
$^{241}\mathrm{Cf} \rightarrow {}^{237}\mathrm{Cm} + \alpha$	7.6600	$(7/2^-)$	$(5/2^+)$	1	9.07×10^{2}	2.04×10^{1}	0.022
$^{242}\mathrm{Cf} \rightarrow {}^{238}\mathrm{Cm} + \alpha$	7.5170	0^+	0^+	0	2.78×10^{2}	5.64×10^{1}	0.203
$^{243}\mathrm{Cf} \rightarrow {}^{239}\mathrm{Cm} + \alpha$	7.4200	$(1/2^+)$	$(7/2^-)$	3	4.59×10^{3}	8.40×10^{2}	0.183
$^{244}\mathrm{Cf} \rightarrow {}^{240}\mathrm{Cm} + \alpha$	7.3289	0^+	0^+	0	1.16×10^{3}	2.78×10^{2}	0.239
$^{245}\mathrm{Cf} \rightarrow {}^{241}\mathrm{Cm} + \alpha$	7.2584	$1/2^+$	$1/2^+$	0	7.65×10^{3}	5.08×10^{2}	0.066
$^{246}\mathrm{Cf} \rightarrow {}^{242}\mathrm{Cm} + \alpha$	6.8616	0^+	0^+	0	1.29×10^{5}	2.29×10^{4}	0.179
$^{247}\mathrm{Cf} \rightarrow {}^{243}\mathrm{Cm} + \alpha$	6.4950	$(7/2^+)$	$5/2^+$	2	2.80×10^{7}	1.12×10^{6}	0.040
$^{248}\mathrm{Cf} \rightarrow {}^{244}\mathrm{Cm} + \alpha$	6.3610	0^+	0^+	0	2.88×10^{7}	4.57×10^{6}	0.159
$^{249}\mathrm{Cf} \rightarrow {}^{245}\mathrm{Cm} + \alpha$	6.2961	$9/2^-$	$7/2^+$	1	1.11×10^{10}	1.08×10^{7}	0.001
$^{250}\mathrm{Cf} \rightarrow {}^{246}\mathrm{Cm} + \alpha$	6.1284	0^+	0^+	0	4.13×10^{8}	5.80×10^{7}	0.140
$^{251}\mathrm{Cf} \rightarrow {}^{247}\mathrm{Cm} + \alpha$	6.1770	$1/2^+$	$9/2^-$	5	2.83×10^{10}	4.98×10^{8}	0.018
$^{252}\mathrm{Cf} \rightarrow {}^{248}\mathrm{Cm} + \alpha$	6.2169	0^+	0^+	0	8.61×10^{7}	1.97×10^{7}	0.229
$^{253}\mathrm{Cf} \rightarrow {}^{249}\mathrm{Cm} + \alpha$	6.1260	$(7/2^+)$	$1/2^+$	4	4.96×10^{8}	3.41×10^{8}	0.687
$^{254}\mathrm{Cf} \rightarrow {}^{250}\mathrm{Cm} + \alpha$	5.9270	0^+	0^+	0	1.69×10^{9}	6.56×10^{8}	0.389
$^{248}\mathrm{Fm} \rightarrow {}^{244}\mathrm{Cf} + \alpha$	7.9940	0^+	0^+	0	3.87×10^{1}	5.65×10^{0}	0.146
$^{249}\mathrm{Fm} \rightarrow {}^{245}\mathrm{Cf} + \alpha$	7.7090	$(7/2^+)$	$1/2^+$	4	4.73×10^{2}	3.65×10^{2}	0.772
$^{250}\mathrm{Fm} \rightarrow {}^{246}\mathrm{Cf} + \alpha$	7.5570	0^+	0^+	0	2.00×10^{3}	2.22×10^{2}	0.111
$^{251}\mathrm{Fm} \rightarrow {}^{247}\mathrm{Cf} + \alpha$	7.4251	$(9/2^-)$	$(7/2^+)$	1	1.06×10^{6}	8.16×10^{2}	0.001
$^{252}\mathrm{Fm} \rightarrow {}^{248}\mathrm{Cf} + \alpha$	7.1527	0^+	0^+	0	9.14×10^{4}	8.36×10^{3}	0.091
$^{253}\mathrm{Fm} \rightarrow {}^{249}\mathrm{Cf} + \alpha$	7.1980	$(1/2)^+$	$9/2^-$	5	2.16×10^{6}	7.84×10^{4}	0.036
$^{254}\mathrm{Fm} \rightarrow {}^{250}\mathrm{Cf} + \alpha$	7.3075	0^+	0^+	0	1.17×10^{4}	1.81×10^{3}	0.155
$^{255}\mathrm{Fm} \rightarrow {}^{251}\mathrm{Cf} + \alpha$	7.2397	$7/2^+$	$1/2^+$	4	7.23×10^{4}	1.99×10^{4}	0.275
$^{256}\mathrm{Fm} \rightarrow {}^{252}\mathrm{Cf} + \alpha$	7.0270	0^+	0^+	0	1.17×10^{5}	2.59×10^{4}	0.222
$^{257}\mathrm{Fm} \rightarrow {}^{253}\mathrm{Cf} + \alpha$	6.8635	$(9/2^+)$	$(7/2^+)$	2	8.70×10^{6}	2.38×10^{5}	0.027

TABLE I. (*Continued.*)

Reaction	$Q_\alpha^{\exp}$ (MeV)	J_i^π	J_f^π	$\ell_{\min}$	$T_{1/2}^{\exp}$ (s)	$T_{1/2}^{\text{calc}}$ (s)	S_α
$^{251}\text{No} \rightarrow {}^{247}\text{Fm} + \alpha$	8.7520	$(7/2^+)$	$(7/2^+)$	0	9.52×10^{-1}	1.01×10^{-1}	0.106
$^{252}\text{No} \rightarrow {}^{248}\text{Fm} + \alpha$	8.5490	0^+	0^+	0	3.49×10^{0}	4.29×10^{-1}	0.123
$^{253}\text{No} \rightarrow {}^{249}\text{Fm} + \alpha$	8.4140	$(9/2^-)$	$(7/2^+)$	1	1.22×10^{2}	1.37×10^{0}	0.011
$^{254}\text{No} \rightarrow {}^{250}\text{Fm} + \alpha$	8.2260	0^+	0^+	0	5.67×10^{1}	4.83×10^{0}	0.085
$^{255}\text{No} \rightarrow {}^{251}\text{Fm} + \alpha$	8.4280	$1/2^+$	$(9/2^-)$	5	7.04×10^{2}	1.32×10^{1}	0.019
$^{256}\text{No} \rightarrow {}^{252}\text{Fm} + \alpha$	8.5810	0^+	0^+	0	2.93×10^{0}	2.98×10^{-1}	0.102
$^{257}\text{No} \rightarrow {}^{253}\text{Fm} + \alpha$	8.4770	$(7/2^+)$	$(1/2)^+$	4	2.50×10^{1}	3.57×10^{0}	0.143

The behavior and value of S_α for odd isotopes in the N variation range $127 \leqslant N \leqslant 135$ are exactly the same in Figs. 3 and 4 due to the similarly of spins of the odd neutron isotopes in this neutron range. Due to this similarity of S_α in the two figures, we expect that the odd isotones for each N value in Fig. 3 have the same spins as the corresponding isotones in Fig. 4. Since some of nuclear spins in this range is either not available or not precisely determined, we try to determine spins based on the correlation between the behavior of S_α and energy levels. For each neutron number in the range $127 \leqslant N \leqslant 135$, we expect the spin of the element Ra is equal to the spin of Th with the same neutron number. For example, J^π for ^{221}Ra is the same as J^π for ^{223}Th and J^π for ^{223}Ra is the same as J^π for ^{225}Th which is equal to $3/2^+$. Moreover, due to the similar behavior of S_α for even N isotopes of the elements Ra and Th on Figs. 3 and 4, respectively, we can expect that the spin of Ac isotopes with even neutron number in the range $126 \leqslant N \leqslant 136$ is the same as Pa isotopes with the same number of neutrons. For example, J^π for ^{215}Ac is the same as J^π for ^{217}Pa and J^π for ^{217}Ac is the same as J^π for ^{219}Pa which is equal to $9/2^-$. Similarly the spin of each Pa isotope with even neutron number in the range $126 \leqslant N \leqslant 140$ is equal to the spin of Np isotope having the same number of neutrons. This is because of the almost similar behavior of S_α for Th element (Fig. 4) and the same quantity for U isotopes appearing on Fig. 5.

Figures 6 and 7 present the variation of S_α with the neutron number for the elements Pu and Cm, respectively. The fast variation of S_α shown in these figures reflects instability of both neutron and proton levels against α emission. Figures 8–10 are for the elements Cf, Fm, and Mo, respectively. The figures indicate a shallow minimum at $N = 152$ showing that this neutron number is a neutron submagic number [3,11], this is confirmed by almost regular variations of S_α in these figures. Figures 8 and 9 show that the preformation probability, S_α, for even number isotopes in the neutron number range $148 \leqslant N \leqslant 156$ have almost similar behavior, this indicates the equality of J^π for Es and Md elements with equal number of neutrons falling in the above range. For example, J^π for ^{253}Es is equal to J^π for ^{255}Md and J^π for ^{251}Es is equal to J^π for ^{253}Md. Considering Figs. 9 and 10, the behavior of S_α for odd N isotopes of the elements Fm and Mo ($N = 149, 151, 153, 155$) is almost the same. Thus, based on our above discussion J^π for ^{249}Fm is equal to J^π for ^{251}Mo and J^π for ^{251}Fm is equal to J^π for ^{253}Mo.

For neutron number with value less than the neutron magic number $N = 126$, Figs. 1–4 show almost similar behavior of S_α with decreasing the number of neutrons. The spin of each of four elements Po, Rn, Ra, and Th with neutron number $N = 125$ is $1/2^-$ which shows that two neutrons at the top of the closed shell lie in the level $3p_{1/2}$. Below this level is the neutron level $5/2^-$, this is confirmed by the spin of Po,

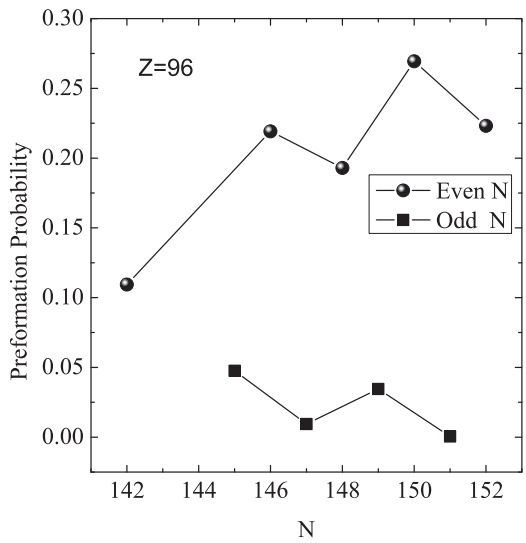

FIG. 7. The same as Fig. 1 but for $Z = 96$.

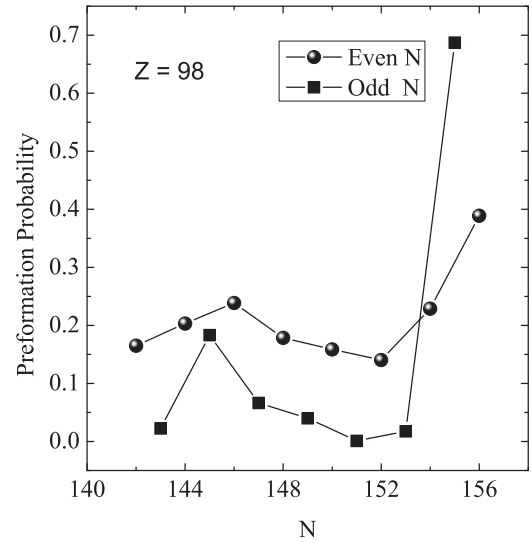

FIG. 8. The same as Fig. 1 but for $Z = 98$.

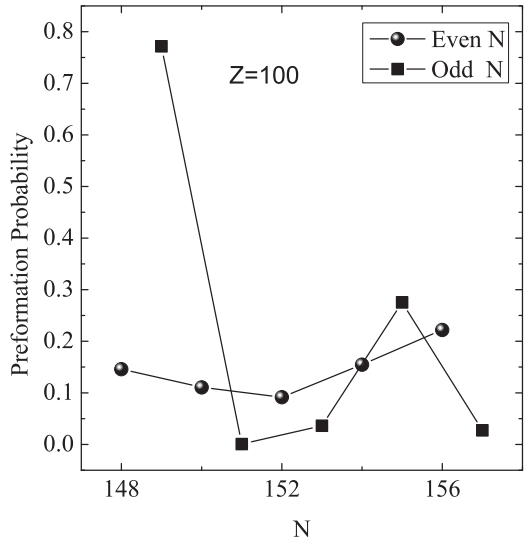

FIG. 9. The same as Fig. 1 but for $Z = 100$.

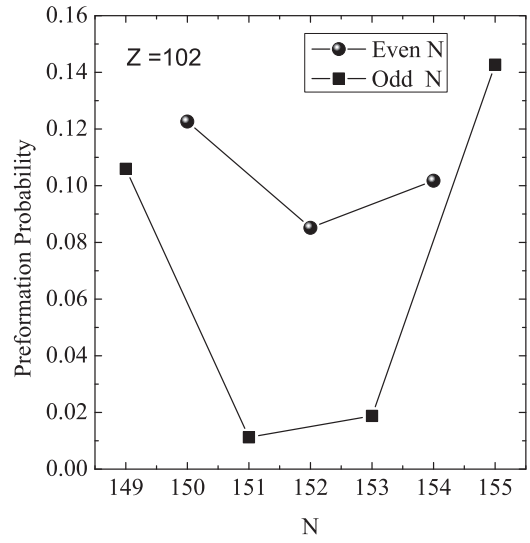

FIG. 10. The same as Fig. 1 but for $Z = 102$.

Rn, and Ra isotopes with neutron numbers $N = 123, 121$, and 119, all these isotopes of the the three elements have spin $5/2^-$. The behavior of S_α in Figs. 1, 2, and 3 as N decreases from $N = 124$ to $N = 120$ is almost the same. This shows that the level $5/2^-$ emits its six neutrons in the emission process and S_α increases with the number of holes in this level. This correlation between S_α and the level $5/2^-$ suggests that we expect the existence of $5/2^-$ level for Th isotopes with $120 \leqslant N \leqslant 124$, the behavior of S_α for these isotopes is very similar to that appear in Figs. 1–3. Since the spin of ^{209,211,213}Th is not precisely determined, we expect based on the similarity of the behavior of S_α for this element and other elements that the spin of these three isotopes is $5/2^-$.

As N decreases in the neutron range $110 \leqslant N \leqslant 118$, S_α varies smoothly on Figs. 1 and 2, S_α increases with decreasing the value of N. This variation is similar to the variation of S_α in case of $5/2^-$ level emission, suggests that the neutron pair in α-particle comes out from a single energy level which lies below $5/2^-$ level. The spin of ^{201}Po is precisely determined and its value is $3/2^-$ [44] while the spins of ^{199,197,195}Po are not precisely determined and their values found in Ref. [44] are $3/2^-$. From the behavior of S_α in Figs. 1 and 2, we confirm that the spin of odd isotopes of Po and Rn with neutron number $N = 117$, 119, 121, and 123 is $3/2^-$. Since the level $3/2^-$ is filled by four neutrons, we assume that when the level becomes empty, it is filled again from lower level leaving holes in this level. The contribution of this level to emission process is accompanied by decrease of S_α for even isotopes and a sudden jump in the value of S_α by more than one order of magnitude for odd isotopes compared to the adjacent even isotopes. This sudden jump at $N = 107$ and 109 is due to the creation of a strange proton hole in $3s_{1/2}$ level (the spin of even N isotopes of At element is $9/2^-$ but ^{195}At and ^{193}At have spin $1/2^+$) besides the existence of holes in $13/2^+$ level. The above-mentioned jump in the value of S_α is repeated on Fig. 2 at $N = 108$ and 110, this time for even isotopes while S_α for odd isotopes vary slowly. We mention that the spin of ^{199}Fr is $1/2^+$ and J^π for ^{201}Fr is $9/2^-$ but no value has been found experimentally for ^{197}Fr. We expect that the spin of this isotope is different from $9/2^-$.

IV. CONCLUSION

The α-particle preformation probability is extracted from the experimental α-decay half-life and the penetration probability is obtained from the WKB approximation in combination with the Bohr-Sommerfeld quantization condition. The microscopic α-nucleus potential is numerically constructed in the well-established double-folding model derived from a realistic density-dependent effective BDM3Y1-Paris NN interaction with finite-range exchange force. The main effect of antisymmetrization under exchange of nucleons between the α and the daughter nuclei has been included in the folding model through the finite-range exchange part of the NN interaction.

We studied the variation of S_α with the neutron number of the parent nucleus for ten even-even and odd mass heavy nuclei from Po to No isotopes. Based on the similarity in the behavior of S_α with the neutron number for two adjacent nuclei, we try to determine the unknown or doubted nuclear spins and parities or at least correlate spins of adjacent nuclei.

[1] D. Bucurescu and N. V. Zamfir, Phys. Rev. C **87**, 054324 (2013).
[2] Dongdong Ni and Zhongzhou Ren, Phys. Rev. C **87**, 027602 (2013).
[3] S. Hofmann and G. Munzenberg, Rev. Mod. Phys. **72**, 733 (2000).
[4] P. E. Hodgeson and E. Betak, Phys. Rep. **374**, 1 (2003).
[5] R. G. Lovas, R. J. Liotta, A. Insolia, K. Varga, and D. S. Delion, Phys. Rep. **294**, 265 (1998).
[6] D. Seweryniak, K. Starosta, C. N. Davids, S. Gros, A. A. Hecht, N. Hoteling, T. L. Khoo, K. Lagergren, G. Lotay, D. Peterson, A. Robinson, C. Vaman, W. B. Walters, P. J. Woods, and S. Zhu, Phys. Rev. C **73**, 061301(R) (2006).

[7] Yu. Ts. Oganessian, F. Sh. Abdullin, C. Alexander, J. Binder, R. A. Boll, S. N. Dmitriev, J. Ezold, K. Felker, J. M. Gostic, R. K. Grzywacz *et al*., Phys. Rev. C **87**, 054621 (2013).
[8] Yu. Ts. Oganessian, F. Sh. Abdullin, P. D. Bailey, D. E. Benker, M. E. Bennett, S. N. Dmitriev, J. G. Ezold, J. H. Hamilton, R. A. Henderson, M. G. Itkis *et al*., Phys. Rev. Lett. **104**, 142502 (2010).
[9] Yu. Ts. Oganessian *et al*., Phys. Rev. C **74**, 044602 (2006).
[10] W. M. Seif, Phys. Rev. C **74**, 034302 (2006).
[11] M. Ismail, A. Y. Ellithi, M. M. Botros, and A. Adel, Phys. Rev. C **81**, 024602 (2010).
[12] G. Gamow, Z. Phys. **51**, 204 (1928).
[13] E. U. Condon and R. W. Gurney, Nature **122**, 439 (1928).
[14] G. Wentzel, Z. Phys. **38**, 518 (1926).
[15] B. Buck, A. C. Merchant, and S. M. Perez, Phys. Rev. C **51**, 559 (1995).
[16] S. B. Duarte and N. Teruya, Phys. Rev. C **85**, 017601 (2012).
[17] M. Ismail and A. Adel, Nucl. Phys. A **912**, 18 (2013).
[18] Y. Qian and Z. Ren, Eur. Phys. J. A **49**, 5 (2013).
[19] M. Ismail and A. Adel, Phys. Rev. C **86**, 014616 (2012).
[20] Y. Qian and Z. Ren, Phys. Rev. C **84**, 064307 (2011).
[21] G. Royer, J. Phys. G: Nucl. Part. Phys. **26**, 1149 (2000).
[22] C. Xu and Z. Z. Ren, Nucl. Phys. A **753**, 174 (2005).
[23] V. Yu. Denisov and A. A. Khudenko, Phys. Rev. C **80**, 034603 (2009).
[24] D. S. Delion, S. Peltonen, and J. Suhonen, Phys. Rev. C **73**, 014315 (2006).
[25] S. Peltonen, D. S. Delion, and J. Suhonen, Phys. Rev. C **75**, 054301 (2007).
[26] K. P. Santhosh and B. Priyanka, Phys. Rev. C **87**, 064611 (2013).
[27] K. P. Santhosh, Jayesh George Joseph, and Sabina Sahadevan, Phys. Rev. C **82**, 064605 (2010).
[28] K. Varga, R. G. Lovas, and R. J. Liotta, Phys. Rev. Lett. **69**, 37 (1992).
[29] Madhubrata Bhattacharya, Subinit Roy, and G. Gangopadhyaya, Phys. Lett. B **665**, 182 (2008).
[30] W. M. Seif, M. Shalaby, and M. F. Alrakshy, Phys. Rev. C **84**, 064608 (2011).
[31] G. R. Satchler and W. G. Love, Phys. Rep. **55**, 183 (1979).
[32] M. Ismail and A. Adel, Phys. Rev. C **84**, 034610 (2011).
[33] C. Xu and Z. Ren, Phys. Rev. C **74**, 014304 (2006).
[34] C. Xu and Z. Ren, Phys. Rev. C **73**, 041301(R) (2006).
[35] B. Sinha, Phys. Rep. **20**, 1 (1975).
[36] B. Sinha and S. A. Moszkowski, Phys. Lett. B **81**, 289 (1979).
[37] J. W. Negele and D. Vautherin, Phys. Rev. C **5**, 1472 (1972).
[38] M. Ismail, F. Salah, and M. M. Osman, Phys. Rev. C **54**, 3308 (1996).
[39] M. Ismail, M. M. Osman, and F. Salah, Phys. Rev. C **60**, 037603 (1999).
[40] Dao T. Khoa, Phys. Rev. C **63**, 034007 (2001).
[41] X. Campi and A. Bouyssy, Phys. Lett. B **73**, 263 (1978).
[42] Dao T. Khoa and W. von Oertzen, Phys. Lett. B **342**, 6 (1995).
[43] N. G. Kelkar and H. M. Castaneda, Phys. Rev. C **76**, 064605 (2007).
[44] NuDat2.6, Nuclear Structure and Decay Data, available from http://www.nndc.bnl.gov/nudat2/.